Hindawi
Shock and Vibration
Volume 2022, Article ID 7299041, 10 pages
https://doi.org/10.1155/2022/7299041

Research Article

Strength Distribution and Damage Constitutive Model of Frozen Sand under Rate-Dependent Evolution

Fangnian Song,[1] **Weihao Yang**,[1] **Zhijiang Yang**,[1] **Xin Huang**,[1] **and Baosheng Wang**[2]

[1]*The State Key Laboratory for Geomechanics and Deep Underground Engineering, China University of Mining and Technology, Xuzhou, Jiangsu, China*
[2]*Shanghai Foundation Engineering Group Co., Ltd., Shanghai, China*

Correspondence should be addressed to Fangnian Song; songfn@cumt.edu.cn

Received 23 May 2022; Accepted 20 June 2022; Published 6 July 2022

Academic Editor: He Mingming

Study of the compressive strength and damage constitutive model of frozen sand has an important significance for construction design and prevention-control of soil destabilization damage in frozen soil engineering. In this paper, a new triaxial apparatus was used to carry out a series of triaxial compression tests of frozen sand under different confining pressure and strain rate, based on which a segmental strength criterion is established to describe the damage of microelement strength of frozen sand. Assuming that the microelement strength of frozen sand obeys the Weibull distribution, a statistical damage constitutive model of frozen sand is established by statistics and continuous medium mechanics. Based on the test data, the model parameters were calculated and the relationship between the strength distribution parameters, the strain rate, and the confining pressure was obtained. Finally, the calculated values of the damage constitutive model are compared with the experimental values, and it is found that the model can simulate the stress-strain process curve of frozen sand well and can reflect the transition of the curve from elasto-plasticity to strain-hardening when the strain rate increases from low to high. The results of this study have an important significance in engineering construction of cold regions and artificial ground freezing projects.

1. Introduction

As a special geotechnical material, frozen soil is widely distributed in high latitudes and upper mountains, while the artificial freezing method is often used in the construction of underground structures (mines, subways, etc.); under the action of stress, the internal fracture of frozen soil will be continuously generated, expanded, and penetrated, which is expressed as the damage of the internal structure of frozen soil, and when the damage accumulates to a certain degree, it will lead to the destruction. By analyzing the strength characteristics of frozen soil under different factors and establishing a damage constitutive model that can predict the damage condition of frozen soil, it is of great significance for construction design and instability disaster prevention in the frozen layer [1–3].

Many scholars have studied the factors influencing the compressive strength of frozen sand, such as temperature, confining pressure, and loading rate, these factors are coupled with each other [4–8]. The triaxial compressive strength of frozen sand is strongly influenced by the confining pressure. Chamberlain et al. [9] conducted triaxial shear tests on saturated frozen sand at temperatures of -10°C, the variation of the confining pressure ranged from 0 to 275.6 MPa. By analyzing the experimental results, the variation of shear strength of frozen sand with confining pressure was divided into three stages: (1) increasing with confining pressure, (2) decreasing with the continuing increase of confining pressure, and (3) a small rebound with increasing confining pressure. Li et al. [10] conducted triaxial shear tests on deep artificial frozen soil after consolidation, and then unloading of the confining pressure and the test results showed that the strength of artificial frozen soil under low confining pressure satisfies the Mohr-Coulomb strength criterion and under high confining pressure satisfies the parabolic yield criterion. Ma et al. [11] proposed a

parabolic-shaped strength yield criterion applicable to both high and low confining pressures based on the results of a large number of triaxial strength tests on frozen soils. Several scholars have found that frozen soil exhibits stronger rate dependence than that of ice and soil [12–14]. Haynes et al. [15] investigated the effect of strain loading rate on the compressive strength of frozen sand at -9.4°C, and it was found that the compressive strength of frozen sand was very sensitive to the strain loading rate, the compressive strength of frozen sand increased 10 times during the increase of strain rate from $2.9\times10^{-4}\,s^{-1}$ to $2.9\,s^{-1}$. Yao et al. [16] conducted three strain loading rates and five constant stresses in-plane compression tests on frozen sand and found that the loading rate had a significant effect on the compressive strength, while the damage form of frozen sand was only related to the loading rate. Lee et al. [13] conducted uniaxial compression tests on frozen sand at different temperatures and loading rates and found that the strength and elastic modulus of frozen sand slowed down with increasing loading rates and that the loading rate had little effect on strength at strain rates above 1%/min. However, few laboratory data address the triaxial compressive strength of frozen sand for a comprehensive consideration of strain rates and confining pressure. Therefore, further research is needed to investigate the strength criterion of frozen sand under the combined effect of confining pressure and loading rate.

Many scholars have started to apply the damage constitutive model to the damage analysis of frozen soil, and a series of results have been obtained. Lai et al. [17, 18] developed a stochastic damage constitutive model for warm frozen clay and warm ice-rich frozen clay by applying continuous damage theory and probability. Li [19] proposed a stochastic damage constitutive model on the foundation of a large number of experimental data, in which the axial strain is regarded as a random variable. Based on the hypothesis of strain equivalence, Cao [20] developed a rate-dependent damage equation to describe the damage characteristics of frozen sand. Zhu et al. [21] presented an elastic constitutive model for frozen soil with damage based on the microcosmic mechanics of composite materials. To the best of the authors' knowledge, previous studies of damage evolution in frozen soils have used less experimental data to simulate the state of in situ stress freezing, while considering more single factors and less integrated consideration of the confining pressure and strain loading rates.

In this study, considering the damage as the evolution of microcracks dependent on the strain rate and confining stress, the strain rate is introduced into the damage evolution equation, based on which a coupling constitutive model of frozen soil under loading is constructed. A series of triaxial compression tests on frozen soil are carried out using the triaxial apparatus, and the stress-strain curves of frozen soil under various strain rates and confining stress are obtained. The relationship between the parameters of the frozen sand damage evolution model based on the Weibull distribution, the confining pressure, and loading rate was obtained through the analysis of the experimental results. Combining the influence of the parameters on the model and the characteristics of the stress-strain curve of the frozen sand rupture process, the parameters were reasonably modified, to establish a more realistic frozen sand damage principal constitutive model.

2. Damage Constitutive Model

At present, there are two main ways to establish the damage constitutive model of frozen soil using damage theory, one is based on the principle of energy equivalence of materials before and after damage, the other is based on the principle of material strain equivalence before and after deformation, and the second method is used in this paper. According to Lemaitre's material strain equivalence hypothesis [22], the baseline damage state of frozen sand (freezing completed) is taken as the first damage state in this paper, and the damage of frozen sand when keeping the confining pressure loaded at a certain rate is taken as the final damage state

$$\varepsilon = \frac{\sigma}{E_{CS}} = \frac{\sigma_{CS}}{E}, \tag{1}$$

where σ represents equivalent force and σ_{CS} represents apparent stress.

Using the elastic modulus to define the damage and combining it with Hooke's law yields

$$\begin{aligned} E_{CS} &= E\left(1 - D_{CS}\right) \text{ and} \\ \sigma_{CS} &= \frac{\sigma}{\left(1 - D_{CS}\right)} = E\left(1 - D_{CS}\right)\varepsilon_{CS}, \end{aligned} \tag{2}$$

where D_{CS} is the damage variable under the coupling of loading rate and confining pressure and E is the elastic modulus of the damaged material.

A large number of tests have proved that the damage of frozen soil under triaxial loading conditions is mainly plastic [23–25] when the frozen soil strength criterion is the condition satisfied by its stress state when plasticity starts to appear at a point within the frozen soil. The damage of frozen sand during loading is considered as a continuous process, where internal defects such as pores and fractures are continuously expanded and developed, achieving penetration in some areas, and then forming macroscopic fractures leading to the damage of the specimen. It is not possible to measure the strength of the soil sample at the time of damage in each region precisely, but it is possible to define the probability of damage occurring in each microelement for a given stress level. Liao et al. [26] conducted a large number of triaxial creep tests on frozen soils, comparing the Weibull distribution and the standard normal distribution with the test values and using the A-D test and the K-S test in the analysis of randomly distributed variables showed that the Weibull distribution can better represent the random distribution of the microelement strength of frozen soils. In the study of the mechanical properties of frozen sand damage under triaxial compression, the following assumptions were made:

(1) The material properties of frozen sand are isotropic in the macroscopic sense.

(2) It is assumed that the damage state of the specimen after freezing is completed as the initial damage.

(3) The strength of each microelement of frozen soil obeys the Weibull distribution, and its probability density function is

$$P(F) = \frac{m}{F_0}\left(\frac{F}{F_0}\right)^{m-1} \exp\left[-\left(\frac{F}{F_0}\right)^m\right], \quad (3)$$

where F is the distribution variable of the random distribution of the microelement intensity and m and F_0 are Weibull distribution parameters, which reflect the shape of the distribution curve.

Previous studies have mostly used axial strain to replace the strength of frozen soil microelements, which has the disadvantage of not reflecting well the effect of complex stress states on the strength of frozen soil microelements. In this paper, based on previous studies, the damage criterion of frozen soil is assumed to be as follows:

$$F = f(\sigma) - B = 0, \quad (4)$$

where B is a constant related to frozen sand cohesion and friction.

F reflects the degree of risk of microelement damage and can be considered as the strength of frozen sand microelement. Assuming that the probability of frozen sand microelement damage is $P[f(\sigma)]$, the number of microelement damage under a certain level of loading is N_t, the number of all cells is N, and the number of damaged microelement when loaded to a certain stress level F is as follows:

$$N_t(F) = \int_0^F NP(y)\mathrm{d}y = N\left(1 - \exp\left[-\left(\frac{F}{F_0}\right)^m\right]\right). \quad (5)$$

The damage variable is the ratio of the number of destroyed microelements to the total number of microelements

$$D_{CS} = \frac{N_t}{N} = 1 - \exp\left[-\left(\frac{F}{F_0}\right)^m\right]. \quad (6)$$

This is the established equation for the evolution of frozen sand damage under the action of the confining pressure. The form of the microelement strength expressed $F = f(\sigma')$ depends on the damage mechanism and damage criterion of the frozen sand. In triaxial tests, nominal stresses σ_1, σ_2, σ_3 ($\sigma_2 = \sigma_3$), and strains ε_1 can be measured, and the constitutive model is as follows:

$$\sigma_1 = E\varepsilon_1(1 - D_{CS}) + 2\mu\sigma_3. \quad (7)$$

The coupling of equation (6) yields a damage constitutive model for frozen sand based on the coupling of confining pressure and loading rate.

$$\sigma_1 = E\varepsilon_1 \exp\left[-\left(\frac{F(\sigma)}{F_0}\right)^m\right] + 2\mu\sigma_3. \quad (8)$$

The parameters that need to be obtained experimentally and substituted into the model are μ (Poisson's ratio of frozen soil) and φ (angle of internal friction of frozen soil). The deformation of the principal relationship in equation (8) leads to

$$\frac{\sigma_1 - 2\mu\sigma_3}{E\varepsilon_1} = \exp\left[-\left(\frac{F(\sigma)}{F_0}\right)^m\right]. \quad (9)$$

Taking the logarithm twice for both sides of the equation, we get the following equation:

$$\ln\left[-\ln\left(\frac{\sigma_1 - 2\mu\sigma_3}{E_C\varepsilon_1}\right)\right] = m \ln F(\sigma) + w. \quad (10)$$

Assuming $y = \ln[-\ln(\sigma_1 - 2\mu\sigma_3/E_C\varepsilon_1)]$, $x = \ln F$, and $w = -m \ln F_0$, then equation (10) can be converted into a quadratic equation concerning x and y,

$$y = mx + w. \quad (11)$$

The specific values of m and F_0 can be found by a linear fit using least squares, which further leads to

$$F_0 = \exp\left(-\frac{w}{m}\right). \quad (12)$$

From the above derivation process, it can be seen that the expression of F contains effective stress. For the triaxial shear test of frozen sand, most of the pore water is in the ice phase, resulting in the effective stress measured during shear being closer to the total stress, so the total stress is approximated to be equal to the effective stress to simplify the calculation.

The above paper establishes a frozen sand damage constitutive model based on the coupling of confining pressure and loading rate, the key to its solution lies in the determination of the Weibull distribution parameters F_0 and m. The parameters can be determined by fitting based on the triaxial test results.

Table 1: The physical properties of the samples.

Parameters	G_s	C_U	C_C	e_0	D_r
Value	2.64	1.46	1.00	0.65	0.33

3. Triaxial Compression Test of Frozen Sand

3.1. Materials and Methods. The Strain control method was used in this study, the applied strain rate ranges from 1×10^{-2} to 1 mm/min (1.04×10^{-5} to 1.04×10^{-3} s^{-1}) and the confining pressures are 3, 7, 10, 12, and 15 MPa. All samples were frozen with a temperature of -5°C, and each group of experiments was repeated three times and averaged to ensure the accuracy of the experiment. The sand used for the test is Fujian standard sand and the basic physical properties of sand samples are listed in Table 1.

The specimens were made by the falling sand method, wrapped with PE heat-shrinkable tubes externally, saturated in the pressure chamber and frozen with pressure, and loaded into the simulated ground stress environment according to the set circumferential pressure after the completion of sample making, keeping the pressure constant

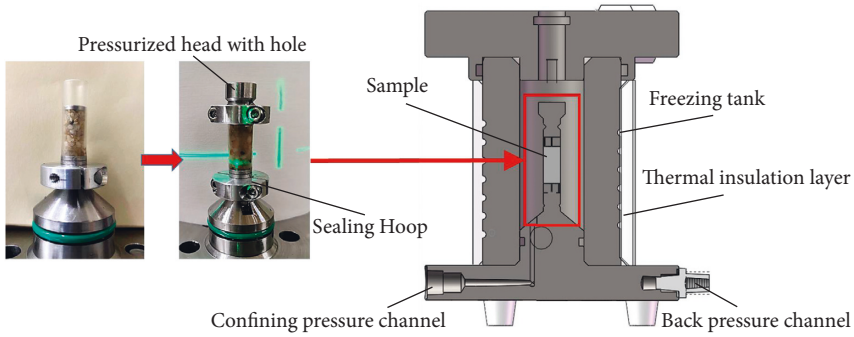

Figure 1: Sand specimen and pressure chamber structure.

and loading according to a certain loading rate after the completion of freezing, as shown in Figures 1 and 2.

It should be noted that the sample size (Φ 8 mm × 16 mm) used in this article is different from the size of the sand sample used in the conventional triaxial test due to the following two reasons:

(1) Many scholars [27–29] have studied the size effect of soil and found that when the aspect ratio of the samples is 2 : 1 and the minimum size is 10 times larger than the maximum particle size, the final test results are less affected by the size of samples

(2) Limitations in the size of the test apparatus used in this paper: the apparatus used was designed to be used for in situ CT scanning during permafrost loading to facilitate comparison with the fine view structures obtained from subsequent CT scans

After the specimen is saturated, the isotropic consolidation is performed on the specimen, the pressure was stabilized until the axial strain rate was less than 0.01 mm/h, the specimen was frozen under pressure for 70 min to make the internal temperature of the specimen uniform. After freezing was completed, it was loaded according to different strain rates and stopped loading at 20% strain rate limit.

3.2. Strength Criterion for Frozen Sand. The deviatoric stress-axial strain curves obtained from the tests are shown in Figure 3. It can be seen that the stress-strain curve of frozen sand at low confining pressure (3 MPa) is ideally elastic-plastic, and the curve form changes to strain hardening as the confining pressure increases to 7 MPa. At high confining pressure ($\sigma_3 > 7$ MPa), the stress-strain relationship is a strain-hardening curve, which is similar to the conclusion obtained by Lai et al. [30] and Ting et al. [12] that there is a boundary confining pressure division, below which the stress-strain form of frozen sand is elastic-plastic or strain-softening, and above which it is strain-hardening.

From the stress-strain relationship curves shown in Figure 3, it can be seen that the stress-strain form and damage strength of frozen sand are strongly influenced by the confining pressure and strain loading rate. When the confining pressure is low, the stress-strain curve shows an ideal elastic-plastic type, and as the confining pressure increases, the curve begins to change to a strain-hardening

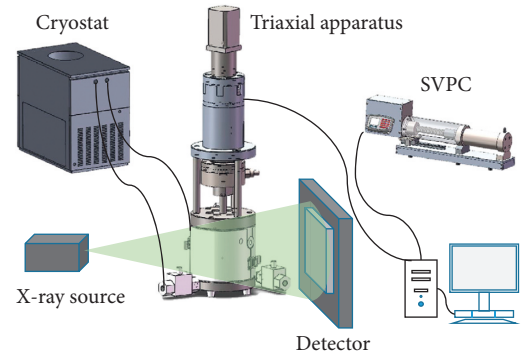

Figure 2: Apparatus used for triaxial tests of frozen sand.

type. Based on the fitting of the experimental data, it was found to be in better agreement with Lai's modified Duncan-Zhang model (2013),

$$\sigma_1 - \sigma_3 = \frac{\varepsilon_1}{m + n\varepsilon_1 + l\varepsilon_1^2}, \tag{13}$$

where m, n, and l are fitting parameters.

Figure 3(e) shows the stress-strain curves and the fitted curves based on equation (13) for the strain loading rate of 1 mm/min and the confining pressure of 3 MPa–15 MPa, and it can be seen from the fitting results that the coefficients of the determination under different confining pressures are greater than 0.95, and the model accuracy is well.

When $\sigma_3 = 3$ MP, there is a maximum value of $\sigma_1 - \sigma_3$, the peak value is taken as the strength of the frozen sand. When $\sigma_3 \geqq 3$ MPa and $\varepsilon_1 < 15\%$, there is no maximum value of $\sigma_1 - \sigma_3$, according to the standard [31], the stress value corresponding to 15% strain is taken as the strength of frozen sand, as shown in Figure 3(f). It can be seen that the triaxial compressive strength of frozen sandy soil increases with the confining pressure, and then decreases when the bounding confining pressure is exceeded, and the whole strength change curve is similar to a parabolic type, so the parabolic frozen sand strength criterion proposed by Ma and Wang [23, 32] is considered to fit

$$q = C + bp - \frac{b}{2p_m}p^2, \tag{14}$$

where

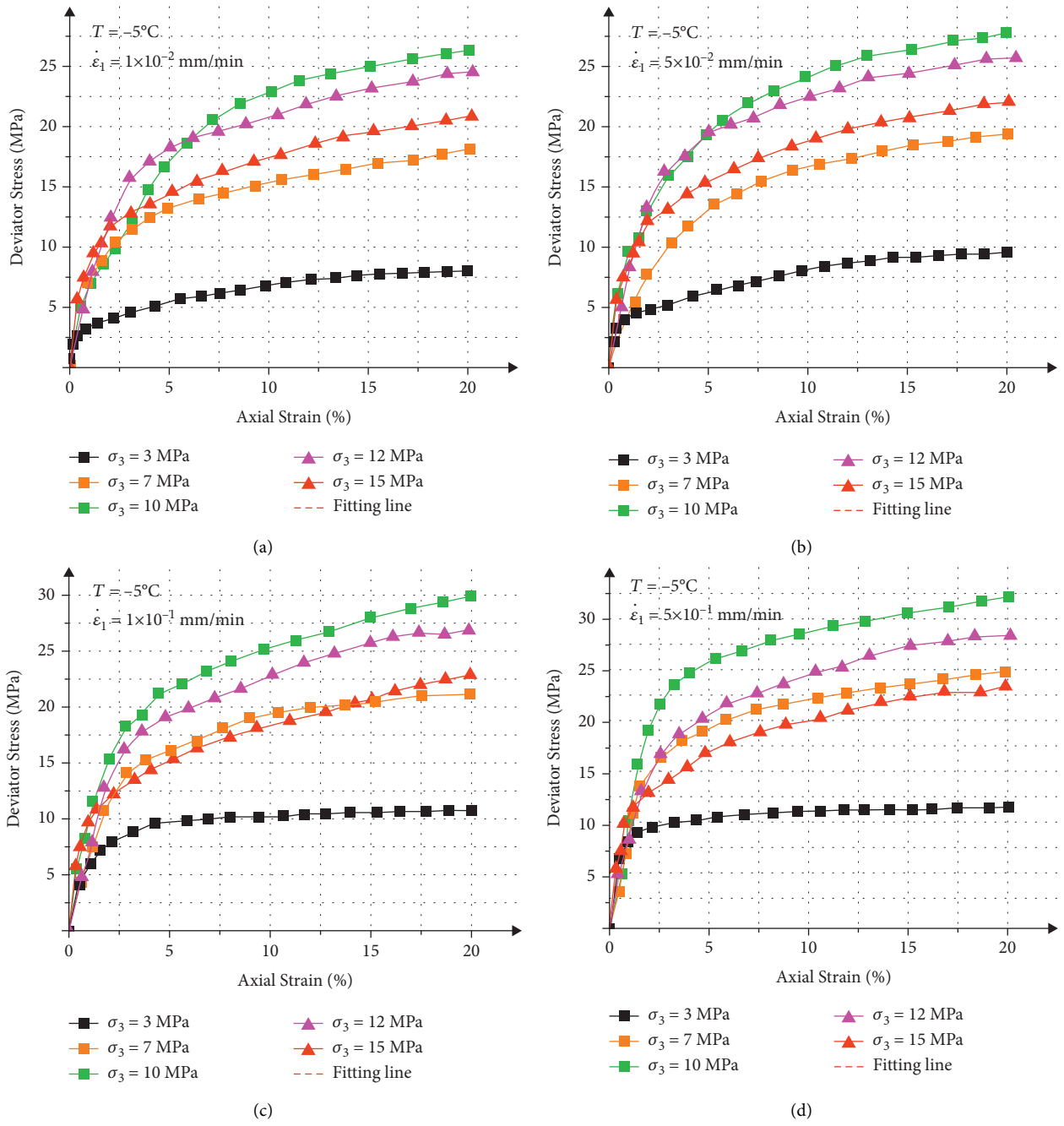

Figure 3: Continued.

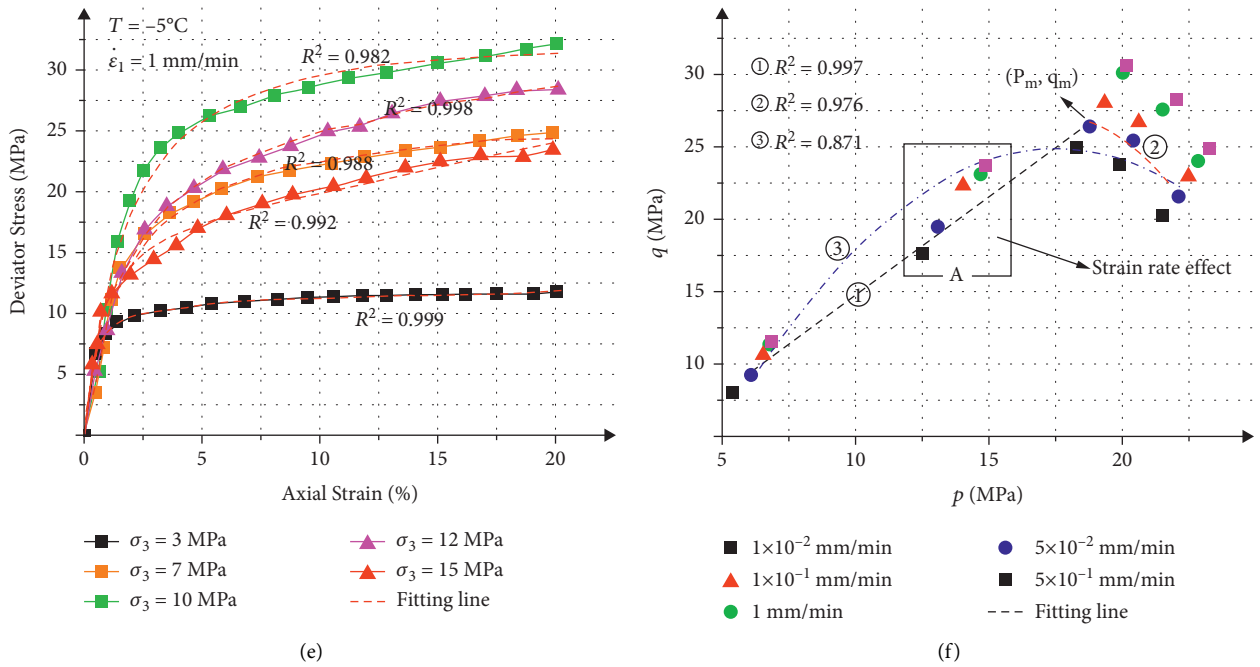

Figure 3: Stress-strain curve and strength change law of frozen sand.

$$\begin{cases} p = \dfrac{1}{3I_1} = \dfrac{1}{3}\left(\sigma_1' + \sigma_2' + \sigma_3'\right) \\ q = \sqrt{3J_2} = \sigma_1' - \sigma_3' \\ b = tg\varphi \end{cases}, \tag{15}$$

where p_m is the average normal stress when the compressive strength of the frozen sand reaches the maximum value q_m, φ is the angle of internal friction, and I_1 and J_2 are the first invariant of the stress tensor and the second invariant of the stress bias, determined from the results of the frozen sand compression tests.

After fitting, it is found that equation (14) fits the test data better at high perimeter pressure (curve ②), with $R^2 \geqq 0.97$ at different loading rates, but deviates more from the test data at $\sigma_3 \leq 10$ MP (curve ③), when the compressive strength of frozen sand is more accurately fitted with the mean normal stress using a linear fit, as shown in line ① (with 5×10^{-2} mm/min as an example).

$$\begin{cases} q = f + kp & \sigma_3 \leq 10\,MPa \\ q = C + bp - \dfrac{b}{2p_m} & p^2\sigma_3 \geq 10\,MPa \end{cases}, \tag{16}$$

where k and f are fitting parameters.

The fitted parameters are shown in Table 2.

Analysis of the fitted parameters reveals that the values of f, k, and C all increase with loading rate, while the opposite is true for the value of b. The fitting of each parameter for the loading rate is shown in Figure 4.

Table 2: Fitting results for each parameter.

	f	k	C	b
1×10^{-2}	1.04	1.31	−69.23	10.78
5×10^{-2}	1.32	1.35	−50.07	8.82
1×10^{-1}	2.06	1.37	−44.01	8.33
5×10^{-1}	1.88	1.43	−35.11	7.71
1	1.86	1.42	−39.3	8.12

From Figure 4, it can be seen that each parameter shows a significant positive or negative correlation with the loading rate during the loading rate of 1×10^{-2}–5×10^{-1} mm/min. When the loading rate is $\dot{\varepsilon}_1 \geqq 5 \times 10^{-1}$ mm/min, the parameters remain unchanged and the sensitivity to the loading rate decreases, this coincides with area A in Figure 3(f). The compressive strength of frozen sand increases with the loading rate in a certain range when the confining pressure is the same, and after reaching a loading rate threshold, it behaves insensitively to the increase of the loading rate. The strength criterion of frozen sand considering the effects of loading rate and confining pressure is obtained, and the microelement strength of frozen sand based on the strength criterion is as follows:

$$F(\sigma) = \begin{cases} \sqrt{3J_2} - \dfrac{1}{3}kI_1 - f & \sigma_3 \leq 10MPa \\ \dfrac{1}{3}I_1 \tan\varphi - \dfrac{\tan\varphi}{18p_m}I_1^2 + \sqrt{3J_2} + C & \sigma_3 > 10MPa \end{cases}, \tag{17}$$

where

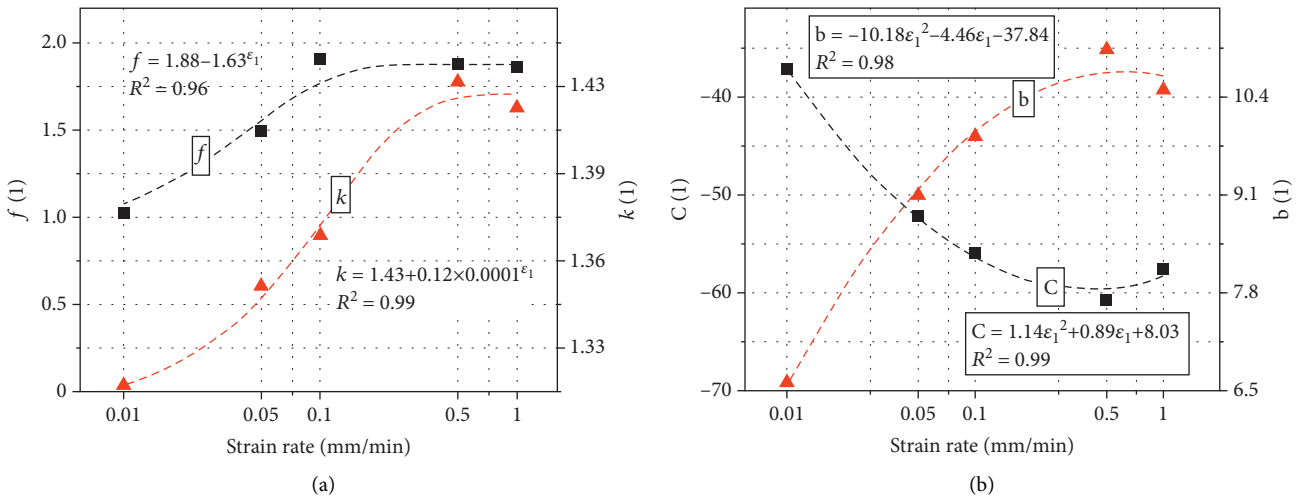

Figure 4: Relationship between each strength parameter and strain loading rate.

$$\begin{cases} f = 1.88 - 1.63^{\dot{\varepsilon}_1} \\ k = 1.43 + 0.12 \times 0.001^{\dot{\varepsilon}_1} \end{cases} \begin{cases} b = -10.18\dot{\varepsilon}_1^{\,2} - 4.46\dot{\varepsilon}_1 - 37.84 \\ C = 1.14\dot{\varepsilon}_1^{\,2} + 0.89\dot{\varepsilon}_1 + 8.03 \end{cases}, \tag{18}$$

where $\dot{\varepsilon}_1$ is the strain loading rate in mm/min.

Transforming I_1 and J_2 yields the following equation:

$$\begin{cases} I_1 = E_0\varepsilon_1 + 2(\mu+1)\sigma_3 \\ J_2 = \dfrac{1}{3}[E_0\varepsilon_1 + 2(\mu-1)\sigma_3]^2 \end{cases}. \tag{19}$$

The microelement strength of permafrost is obtained after substituting in equation (19) as follows:

$$F(\sigma) = \begin{cases} [E_0\varepsilon_1 + 2(\mu-1)\sigma_3] - \dfrac{1}{3}k[E_0\varepsilon_1 + 2(\mu+1)\sigma_3] - f\ \sigma_3 \le 10MPa \\ \dfrac{1}{3}\tan\varphi[E_0\varepsilon_1 + 2(\mu+1)\sigma_3]\left[1 - \dfrac{1}{6P_m}[E_0\varepsilon_1 + 2(\mu+1)\sigma_3]\right] \\ +[E_0\varepsilon_1 + 2(\mu-1)\sigma_3] + C\,\sigma_3 > 10MPa \end{cases}. \tag{20}$$

The damage constitutive model of frozen sand considering the effect of loading rate and confining pressure is obtained by bringing equation (20) in equation (8), where the parameters to be found are E, μ, F_0, m and φ; k, f, and b, and C can be fitted above based on experimental data.

4. Triaxial Compression Test of Frozen Sand

According to the triaxial test data, 1.5% of the axial strain was taken as the linear elastic phase to obtain the elastic constants, such as the elastic modulus and Poisson's ratio. The radial strain of the frozen sand specimen was extremely unevenly distributed along the axial direction after the damage, showing a waist drum-like deformation with large middle and small ends, so when calculating Poisson's ratio by calculating the radial deformation, the strain was calculated by using the average radial strain

$$\Delta V = \Delta V_t - \Delta V_p - \Delta V_L, \tag{21}$$

where ΔV_t is the overall variation measured by the SVPC (volume and pressure control) instrument at t during the shearing process, ΔV_L is the hydraulic oil volume change caused by the intrusion of the loading rod into the pressure chamber, calculated by the intrusion volume of the loading rod, and ΔV_p is the volume change of the hydraulic fluid during unloading at the same pressure without sample.

The correction of the samples area ware calculated according to the following formula:

$$A_t = \frac{V_0 - (\Delta V_t - \Delta V_p - \Delta V_L)}{h_0(1-\Delta\varepsilon_1)}. \tag{22}$$

In data processing, the mean radial strain of samples was modified using the following formula:

$$\overline{\varepsilon_3} = \frac{\sqrt{(A_t/\pi)} - r}{r} = \sqrt{\frac{-(\Delta V_t - \Delta V_p - \Delta V_L) + r^2\pi h\Delta\varepsilon_1}{r^2\pi h(1-\Delta\varepsilon_1)}}, \tag{23}$$

Table 3: Elastic modulus and Poisson's ratio of frozen sand.

$\dot{\varepsilon}_1$ (mm/min)	σ_3 7 MPa			12 MPa		
	E (MPa)	μ (1)	φ	E (MPa)	μ (1)	φ
1×10^{-2}	902.4	0.398	0.57	777.1	0.426	0.62
5×10^{-2}	544.9	0.375	0.58	835.2	0.412	0.61
1×10^{-1}	643.6	0.354	0.58	695.7	0.376	0.57
5×10^{-1}	875.9	0.425	0.61	898.3	0.452	0.63
1	842.8	0.447	0.61	901.0	0.428	0.59

Table 4: Fitting results for the parameters of equations (10) and (12).

$\dot{\varepsilon}_1$ (mm/min)	σ_3 7 MPa		12 MPa	
	F_0	m	F_0	m
1×10^{-2}	21.34	0.54	34.25	0.65
5×10^{-2}	20.86	0.43	30.86	0.50
1×10^{-1}	20.94	0.31	31.21	0.39
5×10^{-1}	19.68	0.33	29.36	0.35
1	19.93	0.34	29.22	0.37

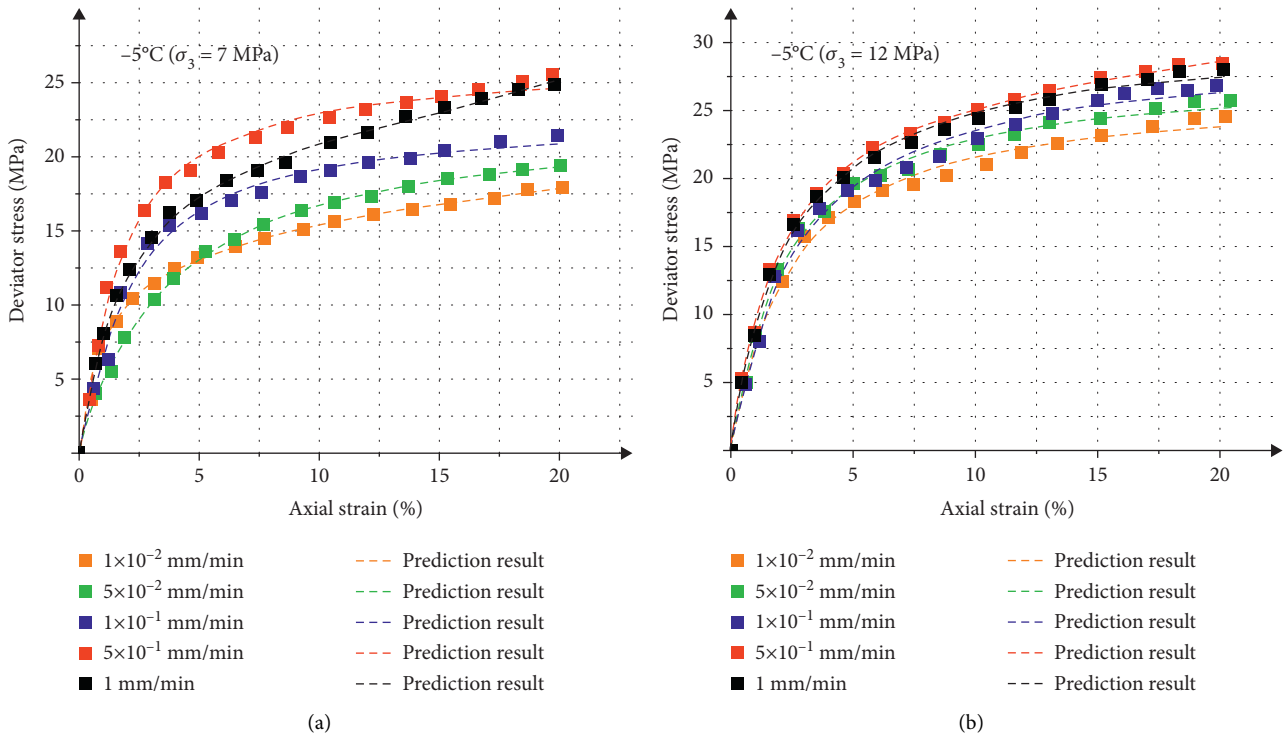

Figure 5: Comparison of calculated and predicted values of stress-strain curves.

where r and h are the initial radius and height of frozen sand, respectively, and ε_1 is the axial strain of the specimen at time t.

Since there are too many tests data, the following calculations are based on the strength criterion of 7 MPa for the linear elastic phase and 12 MPa for the parabolic segment, and the results are shown in Table 3.

Based on the results of triaxial compression tests, the damage constitutive model parameters were determined, and the results are shown in Table 4.

According to equations (10)–(12) and the fitting parameters, the stress-strain prediction curves of frozen sand under different confining pressures and loading rates can be obtained, and the comparison with the experimental results

is shown in Figure 5, from which it can be seen that the damage constitutive model of frozen sand based on the strength criterion of segmentation in this paper can simulate the stress-strain process curves well and has good agreement with the experimental results.

5. Conclusion

In this paper, the effect of confining pressure and strain loading rate on the triaxial compressive strength of frozen sand is investigated by a new designed triaxial apparatus, and the segmental strength criterion of frozen sand is established based on the damage mechanics theory and probabilistic statistical method, and the damage statistical constructive model of frozen sand is established based on the segmental strength criterion assuming that the microelement strength obeys Weibull distribution. The main conclusions are as follows:

(1) In the triaxial compression test, the stress-strain curve of frozen sand transforms from elastic-plastic to strain-hardening type as the confining pressure increases. The loading rate has limited influence on the damage form of frozen sand, mainly affecting the size of its elastic mode and damage strength.

(2) There are thresholds for the effects of both confining pressure and strain rate on the confining pressure of frozen sand. The strength of frozen sand increases with the confining pressure and strain rate at the initial stage, and after it is greater than the threshold value, the increase of confining pressure leads to the decrease of strength, and the increase of strain rate has no obvious effect on the strength.

(3) Based on the p-q curve of the test results, the segmental strength criterion of frozen sand for medium and low confining pressures was established. A damage constitutive model of frozen sand considering the effects of loading rate and confining pressure was established based on the probabilistic theory and strain equivalence principle and compared with the test data with good model accuracy. [33]

Data Availability

All data generated or analyzed during this study are included in this article.

Conflicts of Interest

The authors declare that they have no conflicts of interest.

Authors' Contributions

Fangnian Song performed data curation, formal analysis, and writing; Weihao Yang performed conceptualization, supervision, review, and editing; and Zhijiang Yang, Xin Huang, and Baosheng Wang reviewed and edited the article.

Acknowledgments

This work was supported by theShanghai Science and Technology Committee Rising-Star Cultivating Program (Sailing Program), Grant No. 22YF1418300.

References

[1] W. P. Li and X. Q. Li, "Mechanism of rupture of shaft linings in coal mine areas buried by thick over-soils in East China," *Géotechnique*, vol. 55, no. 3, pp. 237–244, 2005.

[2] Z. Wang, J. Pan, Q. Hou, B. Yu, M. Li, and Q. Niu, "Anisotropic characteristics of low-rank coal fractures in the Fukang mining area," *China. Fuel*, vol. 211, pp. 182–193, 2018.

[3] Z. Wang, X. Fu, M. Hao et al., "Experimental insights into the adsorption-desorption of CH4/N2 and induced strain for medium-rank coals," *Journal of Petroleum Science and Engineering*, vol. 204, Article ID 108705, 2021.

[4] Y. Lai, X. Xu, Y. Dong, and S. Li, "Present situation and prospect of mechanical research on frozen soils in China," *Cold Regions Science and Technology*, vol. 87, pp. 6–18, 2013.

[5] S. Y. Kim, W. Hong, and J. Lee, "Silt fraction effects of frozen soils on frozen water content, strength, and stiffness," *Construction and Building Materials*, vol. 183, pp. 565–577, 2018.

[6] M. Kadivar and K. N. Manahiloh, "Revisiting parameters that dictate the mechanical behavior of frozen soils," *Cold Regions Science and Technology*, vol. 163, pp. 34–43, 2019.

[7] Bo Ma, J. Teng, H. Li, S. Zhang, G. Cai, and D. Sheng, "A new strength criterion for frozen soil considering pore ice content," *International Journal of Geomechanics*, vol. 22, no. 7, 2022.

[8] F. Song, X. Huang, T.-T. Luo, J.-Q. Zou, and R. Fu, "Strain energy evolution and damage characteristics of deep clay under different stress rates," *Journal of Central South University*, vol. 29, no. 5, 2022.

[9] E. Chamberlain, C. Groves, and R. Perham, "The mechanical behaviour of frozen earth materials under high pressure triaxial test conditions," *Géotechnique*, vol. 22, no. 33, pp. 469–483, 1972.

[10] D. Li, J. Fan, and R. Wang, "Research on visco-elastic-plastic creep model of artificially frozen soil under high confining pressures," *Cold Regions Science and Technology*, vol. 65, no. 2, pp. 219–225, 2011.

[11] W. Ma, Z. Wu, L. Zhang, and X. Chang, "Analyses of process on the strength decrease in frozen soils under high confining pressures," *Cold Regions Science and Technology*, vol. 29, no. 1, pp. 1–7, 1999.

[12] J. M. Ting, R. Torrence Martin, and C. C. Ladd, "Mechanisms of strength for frozen sand," *Journal of Geotechnical and Geoenvironmental Engineering*, vol. 10, no. 109, pp. 1286–1302, 1983.

[13] J. Lee, Y. S. Kim, D. Chae, and W. Cho, "Loading rate effects on strength and stiffness of frozen sands," *KSCE Journal of Civil Engineering*, vol. 20, no. 1, pp. 208–215, 2016.

[14] V. R. Parameswaran, "Deformation behaviour and strength of frozen sand," *Canadian Geotechnical Journal*, 1980.

[15] F. D. Haynes, J. A. Karalius, and J. Kalafut, *Strain Rate Effect on the Strength of Frozen silt*, 1975, Crrel Report RR350.

[16] X. Yao, J.-L. Qi, M.-Y. Zhang, and F. Yu, "Strength attenuation effects on rate-dependent law of stress development of frozen sand," *European Journal of Environmental and Civil Engineering*, vol. 24, no. 7, pp. 880–894, 2020.

[17] Y. Lai, S. Li, J. Qi, Z. Gao, and X. Chang, "Strength distributions of warm frozen clay and its stochastic damage

constitutive model," *Cold Regions Science and Technology*, vol. 53, no. 2, pp. 200–215, 2008.

[18] Y. Lai, J. Li, and Q. Li, "Study on damage statistical constitutive model and stochastic simulation for warm ice-rich frozen silt," *Cold Regions Science and Technology*, vol. 71, pp. 102–110, 2012.

[19] S. Li, "An improved statistical damage constitutive model for warm frozen clay based on Mohr–Coulomb criterion," *Cold Regions Science and Technology*, vol. 57, no. 2-3, pp. 154–159, 2009.

[20] C. Cao, "A constitutive model for frozen soil based on rate-dependent damage evolution," *International Journal of Damage Mechanics*, vol. 27, no. 10, pp. 1589–1600, 2018, https://doi.org/10.1177/1056789517741339.

[21] Z. Zhu, J. Ning, and W. Ma, "A constitutive model of frozen soil with damage and numerical simulation for the coupled problem," *Science China Physics, Mechanics & Astronomy*, vol. 53, no. 4, pp. 699–711, 2010, https://doi.org/10.1007/s11433-010-0169-z.

[22] J. Lemaitre, "A continuous damage mechanics model for ductile fracture," *Transactions of the Asme Journal of Engineering Materials & Technology*, vol. 107, no. 107, pp. 83–89, 1985, https://doi.org/10.1115/1.3225775.

[23] D. Wang, "Study on strength of artificially frozen soils in deep alluvium," *Tunnelling and Underground Space Technology*, vol. 23, no. 4, pp. 381–388, 2008, https://doi.org/10.1016/j.tust.2007.06.010.

[24] X. Liu, E. Liu, and D. Zhang, "Study on strength criterion for frozen soil," *Cold Regions Science and Technology*, vol. 161, pp. 1–20, 2019, https://doi.org/10.1016/j.coldregions.2019.02.009.

[25] D. Li, X. Yang, and J. Chen, "A study of Triaxial creep test and yield criterion of artificial frozen soil under unloading stress paths," *Cold Regions Science and Technology*, vol. 141, pp. 163–170, 2017.

[26] M. Liao, Y. Lai, J. Yang, and S. Li, "Experimental study and statistical theory of creep behavior of warm frozen silt," *KSCE Journal of Civil Engineering*, vol. 20, no. 6, pp. 2333–2344, 2016.

[27] R. A. Bragg and O. B. Andersland, "strain rate, temperature, and sample size effects on compression and tensile properties of frozen sand," in *Developments in Geotechnical Engineering*Elsevier, 1982.

[28] M. N. Islam, A. Siddika, M. B. Hossain, A. Rahman, and M. A. Asad, "Effect of particle size on the shear strength behaviour of sands," *Australian Geomechanics Journal*, vol. 46, no. 3, pp. 85–95, 2011.

[29] S. Skuodis, N. Dirgeliene, and I. Lekstutyte, "Change of soil mechanical properties due to triaxial sample size," in *Proceedings of the 13th International Conference Modern Building Materials, Structures and Techniques*, pp. 470–474, Vilnius, Lithuania, May 2019.

[30] Y. Lai, Y. Yang, X. Chang, and S. Li, "Strength criterion and elastoplastic constitutive model of frozen silt in generalized plastic mechanics," *International Journal of Plasticity*, vol. 26, no. 10, pp. 1461–1484, 2010, https://doi.org/10.1016/j.ijplas.2010.01.007.

[31] Astm D4767-11, *Standard Test Method for Consolidated Undrained Triaxial Compression Test for Cohesive Soils*, ASTM D4767-11, 2020.

[32] W. Ma and X. Chang, "Analyses of strength and deformation of an artificially frozen soil wall in underground engineering," *Cold Regions Science and Technology*, vol. 34, no. 1, pp. 11–17, 2002, https://doi.org/10.1016/S0165-232X(01)00042-8.

[33] L. Tang, S. Cong, X. Ling, W. Xing, and Z. Nie, "A unified formulation of stress-strain relations considering micro-damage for expansive soils exposed to freeze-thaw cycles," *Cold Regions Science and Technology*, vol. 153, pp. 164–171, 2018.